


Hydrogen tunes magnetic anisotropy by affecting local hybridization at the interface of a ferromagnet with nonmagnetic metals

Konstantin Klyukin¹, Geoffrey Beach,¹ and Bilge Yildiz^{1,2,*}

¹*Department of Materials Science and Engineering, Massachusetts Institute of Technology, 77 Massachusetts Avenue, Cambridge, Massachusetts 02139, USA*

²*Department of Nuclear Science and Engineering, Massachusetts Institute of Technology, 77 Massachusetts Avenue, Cambridge, Massachusetts 02139, USA*

 (Received 6 May 2020; revised 10 August 2020; accepted 15 September 2020; published 28 October 2020; corrected 1 April 2021)

Ionic control of magnetic properties, dubbed magneto-ionics, has gained much attention in recent years due to the sizable effects that can be induced by electrically controlled ion motion. Here we assess the mechanism by which hydrogen affects magnetic anisotropy in representative ferromagnetic/nonmagnetic metal layers. We take Co/Pd film as a model system that is widely used in spintronics. First-principles calculations demonstrate that the magnetic moment can be switched by 90° via hydrogen insertion at the Co/Pd interface. This control results from hydrogen-induced changes in magnetic anisotropy originating from modifications to the electronic structure. Accumulation of hydrogen at the Co/Pd interface affects the hybridization between neighboring Co and Pd layers, leading to a decrease of the perpendicular anisotropy component, and eventually changes the net magnetic anisotropy to in-plane. Hydrogen penetration into the interior Co layers has the opposite effect, promoting perpendicular magnetic anisotropy. These changes are governed by competing contributions of the d_{xy} ; $d_{x^2+y^2}$ and the $3d_{z^2}$; $3d_{xy}$ states, which are mainly responsible for the perpendicular and the in-plane magnetocrystalline anisotropy, respectively. By using this understanding, we predict that hydrogen accumulation at Fe/V interfacial layers causes the opposite spin reorientation effect, promoting perpendicular magnetic anisotropy.

DOI: [10.1103/PhysRevMaterials.4.104416](https://doi.org/10.1103/PhysRevMaterials.4.104416)

I. INTRODUCTION

Magnetic anisotropy is one of the key properties of magnetic materials that determines a preferred spin orientation and switching dynamics. The ability to manipulate magnetization direction plays a crucial role in the development of spintronics, including emerging spin-transfer [1] and spin-orbit torque [2] memory devices. Therefore, new strategies to control magnetic anisotropy are in high demand. Previous investigations demonstrated several ways to alter magnetization direction by using applied mechanical stress [3], electric field [4,5], electric polarization [6], or adsorption of chemicals [7].

Much of the recent studies have focused on the electrical field control of magnetic anisotropy [8–10] in ferromagnetic/heavy metal [11] and ferromagnetic/metal oxide [12] multilayers. These materials exhibiting perpendicular magnetic anisotropy (PMA) have traditionally gained a lot of attention for practical applications such as high-density magneto-optical recording media [13]. Perpendicular magnetic anisotropy in these films originates from the spin-orbit-coupling (SOC) interaction at the interface, while magnetic anisotropy switching occurs due to modulation of the electronic structure by applying an electric field [14]. However, the direct effect of an electric field in metallic layers is quite small [4] because of the strong Coulomb screening, which significantly limits the energy efficiency of this method.

More recent investigations [10,15–17] have opened an alternative mechanism for low-power gate-voltage switching of magnetization. This approach relies on the electrical gating of mobile ionic species such as oxygen or hydrogen defects to effectively manipulate the interfacial magnetic anisotropy. For instance, it was shown that electrical gating to insert/extract hydrogen allows for reversible switching of magnetic anisotropy in thin films made of ferromagnet and nonmagnetic metal layers, such as Co/Pd [17]. At ambient conditions, these films show an easy magnetization axis that is perpendicular to the film plane, while after hydrogen insertion, magnetization undergoes a 90° rotation to become in-plane. The applicability of a Co/Pd heterostructure as low-pressure hydrogen sensors has also been recently demonstrated based on the H₂-dependent variation of magnetic anisotropy observed through ferromagnetic resonance [18,19] or magneto-optic Kerr effect measurements [20]. In addition to magnetic anisotropy, hydrogenation of magnetic structures was employed to manipulate noncollinear magnetic states by reversibly tuning the Dzyaloshinskii-Moriya interaction [21,22] and stabilizing the formation of skyrmions (e.g., at the Fe/Ir interface [23,24]).

Previous investigations demonstrated that the effect of hydrogen intercalation on the magnetic properties varies with hydrogen concentration and synthesis conditions. The underlying mechanism of magnetic anisotropy changes in relation to the concentration and position of hydrogen is not yet completely understood. In particular, a large set of experimental investigations demonstrated that H₂ absorption leads

*Corresponding author: byildiz@mit.edu

to a reduction of PMA for nanopatterned Co/Pd films, alloys, and multilayers [19,25]. It was hypothesized that the reduction of PMA could be attributed to magnetoelastic effects or modification of the electronic structure and orbital moments at the interface [26,27]. However, other studies revealed an enhancement of PMA and coercivity for multilayered Pd/Co nanopatterns [28] and alloys [29], at low hydrogen concentrations.

To provide a mechanistic understanding of how hydrogen induces changes in magnetic anisotropy, and thus to advance our ability to control it, atomistic scale and theoretical calculations are desirable. In the present work, we have performed density functional theory calculations to assess the mechanisms by which hydrogen affects the magnetic properties of Co/Pd heterostructures. Our calculations have revealed that hydrogen atoms accumulated at the interface modify the strength of magnetic anisotropy through the modulation of electronic d states. The resulting magnetic properties are affected by hydrogen concentration and distribution profiles. Furthermore, we showed that hydrogen gating could be applied to manipulate the magnetic properties of other materials such as Co/Pt, Fe/Pd, and Fe/V thin films.

II. COMPUTATIONAL METHODS

Density functional theory (DFT) calculations were performed using the projector augmented wave (PAW) method as implemented in VASP [30]. We employed the gradient-corrected exchange-correlation functional of the Perdew-Burke-Ernzerhof revised for solids (PBEsol) [31]. An energy cutoff of 500 eV and $12 \times 12 \times 1$ k -point sampling were used for atomic relaxations in the absence of spin-orbit coupling (SOC) until the Hellmann-Feynman forces on each atom became less than 5 meV/Å. The calculated Co/Pd model was composed of 4 Co layers sandwiched between 14 Pd layers at both sides. In accordance with experimental data, we assumed an epitaxial growth of fcc Co on an [111] Pd substrate [32]. The in-plane lattice constant a of the supercell was constrained to bulk fcc Pd, $a = 3.871$ Å. The out-of-plane lattice constant as well as other atomic coordinates were fully relaxed. Hydrogen atoms are found to be stable at the octahedral interstitial Pd and Co lattice sites. To simulate a wide range of hydrogen concentrations, we used a 3×3 supercell with hydrogen atoms randomly distributed across the Co/Pd layers. Similar models were generated for (111) Co/Pt, (100) Fe/(110) Pd, and (100) Fe/V trilayers, assuming an epitaxial growth of magnetic layers on nonmagnetic metal substrates. Additional details can be found in the Supplemental Material [45].

Two sources contributing to the magnetic anisotropy of the Co/Pd thin film are considered: magnetocrystalline anisotropy (MCA) and magnetic shape anisotropy (MSA). The first contribution is associated with electronic effects at Co/Pd interfaces and derived directly from DFT calculations including spin-orbit-coupling effects. Fully self-consistent calculations of magnetic anisotropy energy are very computationally demanding. Thus, we have first examined the accuracy of non-self-consistent approaches [33], such as many-body second-order perturbation treatment of the SOC effect and force theorem, to evaluate magnetic anisotropy

energy. We have found that non-self-consistent methods demonstrate reasonable accuracy to describe SOC effects in the Co/Pd system (see Table S2 in the Supplemental Material [45]), while the use of the fully self-consistent approach is necessary for Co/Pt layers. Therefore, we used non-self-consistent methods for the Co/Pd calculations described in Secs. III A and III B, and fully self-consistent calculations including SOC effects for the calculations of various metallic trilayers discussed in Sec. III D. Both the fully self-consistent and the non-self-consistent calculations were performed using a $24 \times 24 \times 2$ k -point sampling. The accuracy of the magnetic anisotropy energy calculations was validated by running simulations with a finer mesh of $36 \times 36 \times 3$ k point, which results in a change of the magnetic anisotropy energy of less than 0.04 meV. Atom-resolved contributions to MCA are evaluated based on second-order perturbation theory [34],

$$E_{MCA} \propto \sum_k \sum_{o,u} \frac{|\langle \mathbf{k}o | L_z | \mathbf{k}u \rangle|^2 - |\langle \mathbf{k}o | L_x | \mathbf{k}u \rangle|^2}{\varepsilon_{ku} - \varepsilon_{ko}}, \quad (1)$$

where $\mathbf{k}o$ and $\mathbf{k}u$ specify the occupied and unoccupied states with the wave vector \mathbf{k} , L_x and L_z are angular momentum operators, and ε_{ku} , ε_{ko} are the orbital energies. In this work, we also refer to the Bruno model, which describes a correlation between magnetocrystalline anisotropy and orbital moments for transition-metal atoms [35] and multilayered systems [36]. In the latter case, if exchange splitting is small and spin-flip terms can be neglected, orbital moment anisotropy becomes proportional to the MCA energy.

The second magnetic anisotropy term originates from a classical magnetostatic (dipolar) interaction and is associated with the shape of the magnetic sample. It was calculated numerically based on DFT optimized structures and magnetic moments using the following equation and cutoff radius of 150 Å:

$$E_{MSA} \propto \sum_{i \neq j} \left[\frac{\mathbf{m}_i \cdot \mathbf{m}_j}{r_{ij}^3} - 3 \frac{(\mathbf{m}_i \cdot \mathbf{r}_{ij}) \cdot (\mathbf{m}_j \cdot \mathbf{r}_{ij})}{r_{ij}^5} \right]. \quad (2)$$

The magnetocrystalline anisotropy and magnetic shape anisotropy energies are calculated as a difference between energies corresponding to the magnetization in the in-plane and out-of-plane directions [e.g., $E_{MCA} = (E_{\perp} - E_{\parallel})/S$]. Therefore, a negative (positive) value of MAE indicates the out-of-plane (in-plane) easy axis.

III. RESULTS AND DISCUSSIONS

A. The origin of PMA in Co/Pd layers

We first investigated magnetic anisotropy at a pristine Co/Pd interface and further used these results as a reference to understand the origin of magnetic anisotropy changes after hydrogen insertion. In accordance with previous experimental data [32], our calculations showed that Co/Pd trilayers exhibit pronounced magnetocrystalline anisotropy (MCA) with -1.82 mJ/m² energy favoring the perpendicular orientation of magnetic moments. The magnetic moment on Co atoms is found to be in the range of 1.76–1.86 μ_B , while adjacent Pd also acquires a weak magnetization corresponding to 0.28 μ_B per atom, which decays fast with decreasing proximity to the interfacial Co layers [see Fig. 1(a)]. The local orbital moments

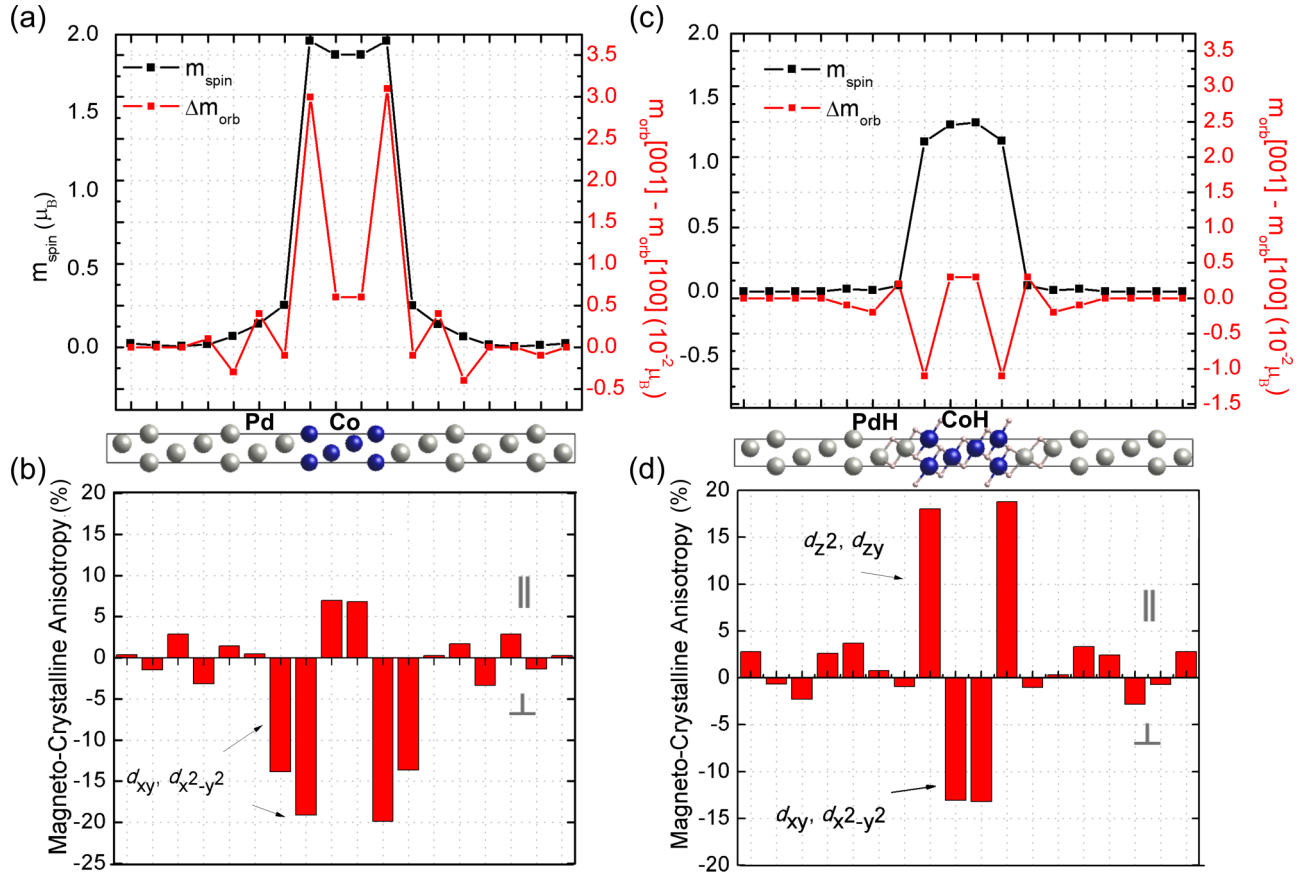


FIG. 1. (a),(c) Layer-resolved magnetic and orbital moments and (b),(d) contributions to magnetocrystalline anisotropy (MCA) for hydrogen-free and hydrogenated Co/Pd thin films as shown in the middle panel. Orbital-resolved contributions are shown for interfacial atoms. Co atoms: blue; Pd atoms: gray; H atoms: pink.

of Co atoms at the interface have a strong anisotropy [see Fig. 1(a)] with an orbital moment $m_{\text{orb}} = 0.092 \mu_B$ for the in-plane and $0.123 \mu_B$ for the perpendicular magnetization orientation. These results agree well with the Bruno model [35,36], which predicts a linear correlation between orbital and magnetic anisotropies for systems with a low spin-flipped contribution such as Co/Pd [37].

The important insights into the origin of MCA can be obtained using second-order perturbation theory, which relies on the electronic structure near the Fermi level [34]. As seen from Fig. 1(b), interfacial Co and Pd layers strongly promote perpendicular magnetic anisotropy, which originates from hybridization between $3d$ Co and $4d$ Pd orbitals. In particular, $d_{x^2-y^2}$ and d_{xy} orbitals of interfacial Co and Pd atoms give the largest contribution to magnetic anisotropy, in agreement with the previous theoretical analysis [37].

Another very important impact on magnetic anisotropy arises from the dipole-dipole interaction of magnetic moments, giving rise to magnetic shape anisotropy. To mimic a planer trilayer of Pd/Co/Pd used in experiments [17], we employed a Co/Pd supercell with a fixed number of Co layers along the z direction and an infinite number of layers along the x and y directions. This model estimates a shape anisotropy energy of 0.58 mJ/m^2 that favors an in-plane orientation of the magnetic moments. Therefore, the total magnetic anisotropy energy (MAE) calculated as a sum

of magnetocrystalline and shape contributions is equal to -1.24 mJ/m^2 for four layers of Co.

Increasing the number of Co layers diminishes the absolute value of MAE, causing anisotropy reorientation in thicker films, as observed experimentally [32]. The MCA contribution does not show any significant dependence on the number of Co layers, varying in the range of -1.75 to -1.85 mJ/m^2 (see Fig. S1 in the Supplemental Material [45]), which confirms the interfacial origin of PMA. On the other hand, the increased shape anisotropy contribution (-1.73 mJ/m^2 for eight Co layers) becomes dominant for Co layers thicker than $\sim 1 \text{ nm}$.

B. Effect of H insertion on magnetic properties of Co/Pd

To understand the effects of hydrogen insertion on the magnetic properties of Co/Pd thin heterostructures, we first considered a fully hydrogenated Co/Pd interface and further investigated the magnetic properties for various hydrogen concentrations and distribution profiles.

As is seen from Fig. 1(c), hydrogenation of the Co/Pd interface leads to a reduction of the magnetic moments down to 1.31 and $0.03 \mu_B$ for interfacial Co and Pd atoms, respectively. This is in a good agreement with recent experimental studies of hydrogenated Co/Pd alloys [38], where a decreased magnetization was observed after hydride formation. We also

demonstrated that hydrogenation affects the orbital moments of interfacial atoms, reducing perpendicular anisotropy and promoting the in-plane component. In particular, the local orbital moment of interfacial Co reduces to 0.043 and 0.053 μ_B for out-of-plane and in-plane directions, respectively. In accordance with the Bruno model [35,36], an alteration of orbital moment anisotropy causes rotation of the magnetic moments. Our calculations confirm that magnetocrystalline energy changes its sign and becomes equal to 0.57 mJ/m², favoring an in-plane orientation of magnetic moments.

A comparison between the layer-resolved decomposition of magnetocrystalline energy before and after hydrogenation [see Figs. 1(b) and 1(d)] demonstrates that magnetic anisotropy switching is caused by two key changes in the electronic structure. First is the sharply decreased contribution of d_{xy} and $d_{x^2+y^2}$. Second is the dramatically increased occupancy of $3d_{z^2}$ and $3d_{zy}$ Co orbitals at the interface with Pd (see, also, Fig. S2 in the Supplemental Material [45]), which promotes in-plane magnetocrystalline anisotropy. Simultaneously, the reduced magnetic moments diminish the contribution of the shape anisotropy down to 0.32 mJ/m². This leads to a total anisotropy of 0.88 mJ/m² favoring in-plane magnetization. We next show that the effect of hydrogen incorporation into the Co/Pd lattice also depends on the hydrogen distribution and concentration profiles.

C. Hydrogen distribution profiles and concentration effect on magnetic anisotropy of Co/Pd

Since the solubility of hydrogen in bulk Pd layers is known to be considerably higher compared to that in bulk Co [19], we first assumed that hydrogen accumulates in the Pd layers and does not reach the interface with Co. However, in this case, no significant changes of magnetic anisotropy were observed. Our calculations revealed that the change in the electronic structure decays very fast with the distance of the Co/Pd interface to a hydrogen defect. The formation of PdH_x three layers away from the interface with Co does not considerably affect the electronic structure of the interfacial atoms responsible for magnetic anisotropy. Only a small reduction of MAE energy, down to -1.19 mJ/m², is observed, within the uncertainty level of our calculation method.

Although Co does not form a stable hydride at ambient conditions, our calculations revealed that hydrogen uptake of thin Co layers in Co/Pd(111) superlattices could be considerably higher compared to bulk Co. This significant increase of hydrogen solubility in Co arises from the strain state of the absorbing Co lattice in the Co/Pd layers, where Co has a large lattice mismatch of $\sim 9\%$ with Pd. Recent experiments confirmed that four monolayers of Co epitaxially grown on Pd(111) experience a large strain of 4–6%, while a gradual relaxation of the strain takes place for thicker films [39]. Our calculations showed that the absorption energy of H in the fcc Co lattice increases with lattice expansion from -0.02 to -0.49 eV for freestanding strain-free (3.55 Å) and epitaxially strained (3.85 Å) Co layers, respectively (see Fig. S2 in the Supplemental Material [45]). Assuming a coherent epitaxial growth, absorption of H in Co, Pd, and Co/Pd layers appears to be almost homogeneous with an energy difference less than 0.1 eV (see Table S1 in the Supplemental Material [45]).

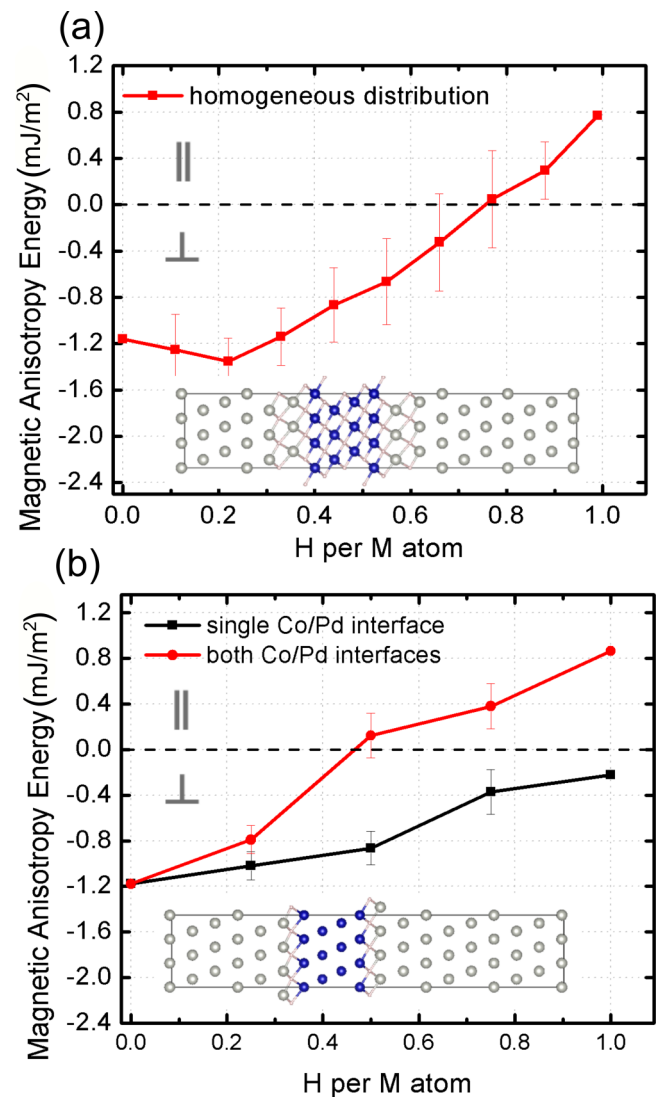


FIG. 2. Magnetic anisotropy energy (MAE) of a Co/Pd trilayer as a function of hydrogen concentration, assuming (a) homogeneous distribution of hydrogen and (b) accumulation of hydrogen at the Co/Pd interface. MAE calculated as an average value of five sampling configurations; error bars correspond to mean-square displacement.

Therefore, we can reasonably assume that hydrogenation of highly textured Co/Pd layers could lead to the formation of CoH_x, similar to what was reported for Co-containing compounds hydrogenated using an arc discharge method [40].

Assuming a homogeneous distribution of hydrogen atoms within the Co/Pd interface, we calculated the dependence of magnetic anisotropy on hydrogen concentration, as shown in Fig. 2(a). At small concentrations, H insertion enhances PMA, leading to MAE of 1.47 mJ/m² for H per metal atom (H/M) equal to 0.2. On the other hand, larger concentrations of hydrogen provoke reduction of PMA and eventually causing anisotropy switching at concentrations of ~ 0.7 H/M. The nonmonotonic dependence of the magnetic properties on H concentration is caused by competing contributions arising from two factors: H atoms at the interface and hydrogenation of the interior Co layer. We found that hydrogen insertion

at the interface between Co and Pd atoms diminishes PMA, affecting hybridization between $4d$ Pd orbitals and $3d$ orbitals of Co as described above. Hydrogenation of interior Co produces the opposite effect. These findings can help to reconcile the contradicting experimental data, where both PMA enhancement and reduction were observed depending on hydrogen concentration and material texture [28,29].

While the assumption of epitaxial growth is an appealing theoretical idealization, real Co films show some deviations from perfect epitaxial growth [32,39]. The substantial lattice mismatch may cause an introduction of interfacial dislocations to reduce the stress in interior Co planes. To address this scenario, we considered accumulation of hydrogen atoms only at the Co/Pd interface.

As is seen in Fig. 2(b), hydrogen accumulation at a single interface leads to a significant reduction of PMA. However, anisotropy switching is not observed even for high H concentration due to the significant impact of the second unaffected Co/Pd interface. To achieve anisotropy switching, one has to consider the presence of hydrogen atoms at both Co/Pd interfaces, which could be driven by H diffusion through a thin Co layer as observed experimentally [17]. In this case, anisotropy switching occurs at the moderate H/M concentration of ~ 0.4 – 0.5 . These changes are followed by a reduction of magnetic moment for both Co and Pd atoms in the vicinity of H defects. An absorbed H atom reduces the magnetic moment of the nearest Co atoms by $\sim 0.1 \mu_B$ for a dilute concentration, while a more significant reduction of $0.6 \mu_B$ is observed for a fully hydrogenated Co/Pd interface.

D. Effect of H insertion at the interface of various FM/NM trilayers

Using fully self-consistent calculations including the SOC effect, we carried out a screening of various trilayers made of a ferromagnet (FM= Co or Fe) a nonmagnetic metal (NM= Pd,Pt,V) commonly used in spintronics. We calculated their response to hydrogenation of interfacial layers. We limited our calculations to high hydrogen concentrations and assumed accumulation of hydrogen only at the interface between FM and NM materials, as shown in Figs. S3 and S4 in the Supplemental Material [45].

As is seen in Fig. 3, our calculations predict PMA for Co/Pd, Co/Pt, and Fe/Pd trilayers in accordance with previous experimental studies [13]. The analysis of orbital-resolved contributions (see Fig. S6 in the Supplemental Material [45]) to the magnetocrystalline anisotropy energy of (100) Fe/(110) Pd indicates that out-of-plane anisotropy is governed by a contribution from d_{xy} and $d_{x^2+y^2}$ orbitals similar to the (111) Co/Pd system discussed above. Hydrogen accumulation at the Co/Pt and Fe/Pd interfaces also causes spin reorientation from out-of-plane to in-plane at high hydrogen concentrations, which corresponds to positive MAE values, as shown in Fig. 3. The most pronounced effect was observed for the (100) Fe/(110) Pd trilayer, which demonstrates strong in-plane anisotropy after hydrogenation. Therefore, a relatively small amount of hydrogen at the interface could cause 90° rotation of the Fe magnetic moment, as was recently observed experimentally for Fe/Pd multilayers in a hydrogen atmosphere [41]. While our calculations also predict magnetic

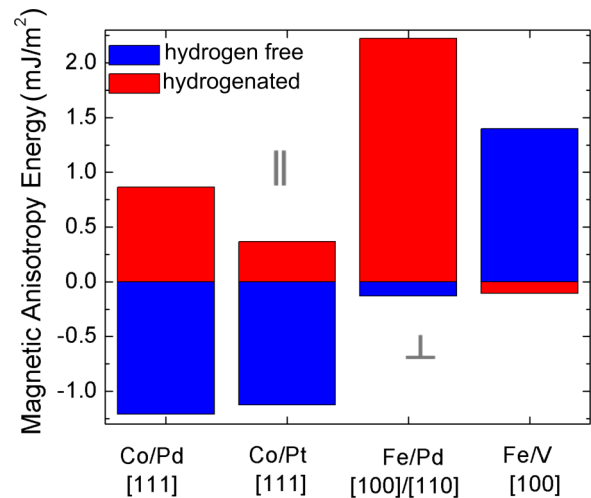


FIG. 3. Magnetic anisotropy energy for various ferromagnetic/nonmagnetic thin-film trilayers before and after hydrogen insertion. The thin-film composition is 4 ML FM/14 ML NM. The magnetocrystalline contribution was calculated using the fully self-consistent approach.

anisotropy switching for Co/Pt, low solubility of H in Pt [42] significantly limits its practical applications.

We have assessed an alternative nonmagnetic metal that has high solubility of hydrogen in its bulk: vanadium [43]. The Fe/V trilayer was chosen as a representative system showing in-plane magnetic anisotropy [44] to investigate the effect of hydrogen insertion. We found that in-plane magnetic moment orientation of 4 ML Fe/14 ML V is driven by both the shape (0.72 mJ/m^2) and in-plane magnetocrystalline anisotropy (0.79 mJ/m^2) components for the hydrogen-free model considered here. In contrast to the Co/Pd trilayers considered above, H absorption in Fe/V promotes perpendicular anisotropy. Our DFT calculations indicate that total magnetocrystalline energy decreases down to -0.88 mJ/m^2 upon hydrogenation, which also correlates with orbital moment anisotropy switching (see Fig. S5 in the Supplemental Material [45]). In spite of slightly increased shape anisotropy of 0.77 mJ/m^2 , the negative total magnetic anisotropy energy of -0.11 mJ/m^2 confines the magnetization to the out-of-plane direction, as shown in Fig. 3. As was discussed above, the main driving mechanism for magnetization switching is a change in the electronic structure near the interface. In the case of Fe/V trilayers, hydrogenation causes an increased contribution from $d_{x^2-y^2}$, d_{xy} orbitals (see Fig. S5 in the Supplemental Material [45]), which promotes perpendicular anisotropy in accordance with second-order perturbation theory [34].

IV. CONCLUSIONS

In summary, using first-principles calculations, we have resolved the effects of hydrogenation on magnetic properties of representative ferromagnet/nonmagnetic metal thin-film trilayers. In particular, we found that anisotropy switching in Co/Pd thin films is associated with a change in the $3d$ Co and $4d$ Pd orbital occupation caused by H intercalation, and both the position and the concentration of hydrogen affect the resulting behavior. First, hydrogen accumulation at

Co/Pd interfaces leads to a reduction of perpendicular magnetic anisotropy and further magnetic anisotropy switching to the in-plane direction. Second, progressive intercalation of hydrogen into the interior Co layers enhances perpendicular magnetic anisotropy. These two competing contributions can explain a nonmonotonic dependence of the magnetic coercive field on hydrogen concentration that was previously observed experimentally [28,29].

Furthermore, we demonstrated that hydrogenation of Co/Pt and Fe/Pd thin-film heterostructures may also cause spin reorientation, leading to in-plane anisotropy. We predict the opposite effect for Fe/V trilayers, which demonstrate a spin reorientation transition from in-plane to out-of-plane after hydrogen insertion. Hydrogenation appears to be a powerful tool to manipulate the magnetic properties of

ferromagnet/nonmagnetic metal layers. Our results advance the understanding of how hydrogen couples to the interface electronic structure locally in manipulating the magnetic anisotropy, and will stimulate further experimental advances.

ACKNOWLEDGMENTS

This work was primarily supported by the National Science Foundation (NSF) through the Massachusetts Institute of Technology Materials Research Science and Engineering Center (MRSEC) under Award No. DMR-1419807. The DFT calculations were carried out using the Extreme Science and Engineering Discovery Environment (XSEDE), which is supported by National Science Foundation Grant No. ACI-1548562 [46].

-
- [1] M. D. Stiles and A. Zangwill, Anatomy of spin-transfer torque, *Phys. Rev. B* **66**, 014407 (2002).
- [2] A. Manchon, J. Železný, I. M. Miron, T. Jungwirth, J. Sinova, A. Thiaville, K. Garello, and P. Gambardella, Current-induced spin-orbit torques in ferromagnetic and antiferromagnetic systems, *Rev. Mod. Phys.* **91**, 035004 (2019).
- [3] D. Sander, The correlation between mechanical stress and magnetic anisotropy in ultrathin films, *Rep. Prog. Phys.* **62**, 809 (1999).
- [4] T. Maruyama, Y. Shiota, T. Nozaki, K. Ohta, N. Toda, M. Mizuguchi, A. Tulapurkar, T. Shinjo, M. Shiraishi, S. Mizukami *et al.*, Large voltage-induced magnetic anisotropy change in a few atomic layers of iron, *Nat. Nanotechnol.* **4**, 158 (2009).
- [5] R. Cherifi, V. Ivanovskaya, L. Phillips, A. Zobelli, I. Infante, E. Jacquet, V. Garcia, S. Fusil, P. Briddon, N. Guiblin *et al.*, Electric-field control of magnetic order above room temperature, *Nat. Mater.* **13**, 345 (2014).
- [6] A. Mardana, S. Ducharme, and S. Adenwalla, Ferroelectric control of magnetic anisotropy, *Nano Lett.* **11**, 3862 (2011).
- [7] N. Tsukahara, K.-I. Noto, M. Ohara, S. Shiraki, N. Takagi, Y. Takata, J. Miyawaki, M. Taguchi, A. Chainani, S. Shin, and M. Kawai, Adsorption-Induced Switching of Magnetic Anisotropy in a Single Iron (ii) Phthalocyanine Molecule on an Oxidized Cu (110) Surface, *Phys. Rev. Lett.* **102**, 167203 (2009).
- [8] F. Matsukura, Y. Tokura, and H. Ohno, Control of magnetism by electric fields, *Nat. Nanotechnol.* **10**, 209 (2015).
- [9] E. Y. Tsybal, Spintronics: Electric toggling of magnets, *Nat. Mater.* **11**, 12 (2012).
- [10] C. Bi, Y. Liu, T. Newhouse-Illige, M. Xu, M. Rosales, J. W. Freeland, O. Mryasov, S. Zhang, S. G. E. te Velthuis, and W. G. Wang, Reversible Control of Co Magnetism by Voltage-Induced Oxidation, *Phys. Rev. Lett.* **113**, 267202 (2014).
- [11] S. Peng, D. Zhu, J. Zhou, B. Zhang, A. Cao, M. Wang, W. Cai, K. Cao, and W. Zhao, Modulation of heavy metal/ferromagnetic metal interface for high-performance spintronic devices, *Adv. Electron. Mater.* **5**, 1900134 (2019).
- [12] B. Dieny and M. Chshiev, Perpendicular magnetic anisotropy at transition metal/oxide interfaces and applications, *Rev. Mod. Phys.* **89**, 025008 (2017).
- [13] F. Hellman, A. Hoffmann, Y. Tserkovnyak, G. S. D. Beach, E. E. Fullerton, C. Leighton, A. H. MacDonald, D. C. Ralph, D. A. Arena, H. A. Durr, P. Fischer, J. Grollier, J. P. Heremans, T. Jungwirth, A. V. Kimel, B. Koopmans, I. N. Krivorotov, S. J. May, A. K. Petford-Long, J. M. Rondinelli, N. Samarth, I. K. Schuller, A. N. Slavin, M. D. Stiles, O. Tchernyshyov, A. Thiaville, and B. L. Zink, Interface-induced phenomena in magnetism, *Rev. Mod. Phys.* **89**, 025006 (2017).
- [14] J. Zhang, P. V. Lukashev, S. S. Jaswal, and E. Y. Tsybal, Model of orbital populations for voltage-controlled magnetic anisotropy in transition-metal thin films, *Phys. Rev. B* **96**, 014435 (2017).
- [15] U. Bauer, L. Yao, A. J. Tan, P. Agrawal, S. Emori, H. L. Tuller, S. Van Dijken, and G. S. Beach, Magneto-ionic control of interfacial magnetism, *Nat. Mater.* **14**, 174 (2015).
- [16] D. A. Gilbert, A. J. Grutter, E. Arenholz, K. Liu, B. J. Kirby, J. A. Borchers, and B. B. Maranville, Structural and magnetic depth profiles of magneto-ionic heterostructures beyond the interface limit, *Nat. Commun.* **7**, 12264 (2016).
- [17] A. J. Tan, M. Huang, C. O. Avci, F. Büttner, M. Mann, W. Hu, C. Mazzoli, S. Wilkins, H. L. Tuller, and G. S. Beach, Magneto-ionic control of magnetism using a solid-state proton pump, *Nat. Mater.* **18**, 35 (2019).
- [18] C. S. Chang, M. Kostylev, and E. Ivanov, Metallic spintronic thin film as a hydrogen sensor, *Appl. Phys. Lett.* **102**, 142405 (2013).
- [19] G. L. Causer, M. Kostylev, D. L. Cortie, C. Lueng, S. J. Callori, X. L. Wang, and F. Klöse, In operando study of the hydrogen-induced switching of magnetic anisotropy at the Co/Pd interface for magnetic hydrogen gas sensing, *ACS Appl. Mater. Interfaces* **11**, 35420 (2019).
- [20] P.-C. Chang, Y.-Y. Chang, W.-H. Wang, F.-Y. Lo, and W.-C. Lin, Visualizing hydrogen diffusion in magnetic film through magneto-optical Kerr effect, *Commun. Chem.* **2**, 89 (2019).
- [21] L. M. Sandratskii and L. Havela, Microscopic nature of drastic influence of hydrogen on the magnetic anisotropy of 5f-electron systems: The case of U₂Ni₂Sn, *Phys. Rev. B* **101**, 100409(R) (2020).
- [22] B. Yang, Q. Cui, J. Liang, M. Chshiev, and H. Yang, Reversible control of Dzyaloshinskii-Moriya interaction at the graphene/Co interface via hydrogen absorption, *Phys. Rev. B* **101**, 014406 (2020).

- [23] P.-J. Hsu, L. Rózsa, A. Finco, L. Schmidt, K. Palotás, E. Vedmedenko, L. Udvardi, L. Szunyogh, A. Kubetzka, K. Von Bergmann *et al.*, Inducing skyrmions in ultrathin Fe films by hydrogen exposure, *Nat. Commun.* **9**, 1571 (2018).
- [24] A. Finco, P.-J. Hsu, K. von Bergmann, and R. Wiesendanger, Tuning noncollinear magnetic states by hydrogenation, *Phys. Rev. B* **99**, 064436 (2019).
- [25] K. Munbodh, F. A. Perez, C. Keenan, D. Lederman, M. Zhernenkov, and M. R. Fitzsimmons, Effects of hydrogen/deuterium absorption on the magnetic properties of Co/Pd multilayers, *Phys. Rev. B* **83**, 094432 (2011).
- [26] K. Munbodh, F. A. Perez, and D. Lederman, Changes in magnetic properties of Co/Pd multilayers induced by hydrogen absorption, *J. Appl. Phys.* **111**, 123919 (2012).
- [27] C. Lueng, P. Lupo, P. J. Metaxas, M. Kostylev, and A. O. Adeyeye, Nanopatterning-enhanced sensitivity and response time of dynamic palladium/cobalt/palladium hydrogen gas sensors, *Adv. Mater. Technol.* **1**, 1600097 (2016).
- [28] W.-C. Lin, C.-J. Tsai, X.-M. Liu, and A. O. Adeyeye, Critical hydrogenation effect on magnetic coercivity of perpendicularly magnetized Co/Pd multilayer nanostructures, *J. Appl. Phys.* **116**, 073904 (2014).
- [29] W.-C. Lin, B.-Y. Wang, H.-Y. Huang, C.-J. Tsai, and V. R. Mudinepalli, Hydrogen absorption-induced reversible change in magnetic properties of Co-Pd alloy films, *J. Alloys Compd.* **661**, 20 (2016).
- [30] G. Kresse and J. Furthmüller, Efficiency of *ab initio* total energy calculations for metals and semiconductors using a plane-wave basis set, *Comput. Mater. Sci.* **6**, 15 (1996).
- [31] G. I. Csonka, J. P. Perdew, A. Ruzsinszky, P. H. T. Philipsen, S. Lebègue, J. Paier, O. A. Vydrov, and J. G. Ángyán, Assessing the performance of recent density functionals for bulk solids, *Phys. Rev. B* **79**, 155107 (2009).
- [32] B. Tudu, K. Tian, and A. Tiwari, Effect of composition and thickness on the perpendicular magnetic anisotropy of (Co/Pd) multilayers, *Sensors* **17**, 2743 (2017).
- [33] M. Blanco-Rey, J. I. Cerdá, and A. Arnau, Validity of perturbative methods to treat the spin-orbit interaction: application to magnetocrystalline anisotropy, *New J. Phys.* **21**, 073054 (2019).
- [34] D.-s. Wang, R. Wu, and A. J. Freeman, First-principles theory of surface magnetocrystalline anisotropy and the diatomic-pair model, *Phys. Rev. B* **47**, 14932 (1993).
- [35] P. Bruno, Tight-binding approach to the orbital magnetic moment and magnetocrystalline anisotropy of transition-metal monolayers, *Phys. Rev. B* **39**, 865 (1989).
- [36] G. van der Laan, Microscopic origin of magnetocrystalline anisotropy in transition metal thin films, *J. Phys.: Condens. Matter* **10**, 3239 (1998).
- [37] J. Okabayashi, Y. Miura, and H. Munekata, Anatomy of interfacial spin-orbit coupling in Co/Pd multilayers using x-ray magnetic circular dichroism and first-principles calculations, *Sci. Rep.* **8**, 8303 (2018).
- [38] S. Akamaru, A. Kimura, M. Hara, K. Nishimura, and T. Abe, Hydrogenation effect on magnetic properties of Pd-Co alloys, *J. Magn. Magn. Mater.* **484**, 8 (2019).
- [39] A. V. Davydenko, A. G. Kozlov, A. V. Ognev, M. E. Steblyi, A. S. Samardak, K. S. Ermakov, A. G. Kolesnikov, and L. A. Chebotkevich, Origin of perpendicular magnetic anisotropy in epitaxial Pd/Co/Pd (111) trilayers, *Phys. Rev. B* **95**, 064430 (2017).
- [40] S.-R. Chung, K.-W. Wang, M.-H. Teng, and T.-P. Perng, Electrochemical hydrogenation of nanocrystalline face-centered cubic co powder, *Intl. J. Hydrogen Energy* **34**, 1383 (2009).
- [41] C.-C. Hsu, P.-C. Chang, Y.-H. Chen, C.-M. Liu, C.-T. Wu, H.-W. Yen, and W.-C. Lin, Reversible 90-degree rotation of Fe magnetic moment using hydrogen, *Sci. Rep.* **8**, 3251 (2018).
- [42] K. Lee, M. Yuan, and J. Wilcox, Understanding deviations in hydrogen solubility predictions in transition metals through first-principles calculations, *J. Phys. Chem. C* **119**, 19642 (2015).
- [43] Y. Fukai, *The Metal-Hydrogen System: Basic Bulk Properties*, Springer Series in Materials Science, Vol. 21 (Springer-Verlag, Berlin, Heidelberg, 2005).
- [44] A. Broddefalk, P. Nordblad, P. Blomquist, P. Isberg, R. Wäppling, O. Le Bacq, and O. Eriksson, In-plane magnetic anisotropy of Fe/V (0 0 1) superlattices, *J. Magn. Magn. Mater.* **241**, 260 (2002).
- [45] See Supplemental Material at <http://link.aps.org/supplemental/10.1103/PhysRevMaterials.4.104416> for more details on first-principles calculations.
- [46] J. Towns, T. Cockerill, M. Dahan, I. Foster, K. Gaither, A. Grimshaw, V. Hazlewood, S. Lathrop, D. Lifka, G. D. Peterson *et al.*, Xsede: Accelerating scientific discovery, *Comput. Sci. Eng.* **16**, 62 (2014).

Correction: Reference [23] contained incorrect source information and has been fixed.